Morphology of martian rampart craters

Peter J. Mouginis-Mark*

Lunar and Planetary Unit, University of Lancaster, Lancaster, UK

Preliminary results from a morphological analysis of the lobate flows around martian rampart craters are presented. The areal dispersal of these deposits displays a proportionally greater maximum range for the lobe as the size of the parent crater increases. It is proposed that lobe formation is not entirely associated with ballistic deposition of the crater's ejecta because the proximal ends of the lobes are found closer to the primary crater rim than to the region of secondary cratering associated with either lunar or mercurian craters. Lobe surface area is shown to be proportional to crater diameter and an estimate of 30–60 m is deduced for the lobe thickness for craters between 10 and 35 km diameter.

The Viking missions to Mars in 1976 provided high resolution photography of many new types of landforms. Of particular interest is a group of craters exhibiting lobate deposits around their rims instead of the normal 'blocky' ejecta blankets observed for lunar and mercurian impact craters[1]. Termed a 'rampart' crater, because of the sharp edge between the distal end of the flow and the surrounding terrain, this type of crater was first observed from Mariner 9 photography[2]. Its unusual character has been attributed either to wind deflation of a ballistically emplaced ejecta blanket[2,3], or the radial movement of a debris flow from the parent crater as a late stage process in the crater-forming event[1,4,5]. A prerequisite in all the debris flow models has been the existence of a layer of ground water or permafrost which lubricates the crater's ejecta after its initial emplacement. Retention of target volatiles, air-layer cushioning as a result of the entrainment of the tenuous martian atmosphere (comparable to the transport mechanism of certain terrestrial landslides[6]) or the incorporation of volatiles during the formation of an impact-generated base surge[7], have all been proposed as possible mechanisms by which the ejecta might increase its mobility in comparison with impact events on the Moon and Mercury[1,4,5].

Possible terrestrial equivalents to these lobate flows have been discussed elsewhere[8]. This paper describes several novel aspects of the morphology of this type of crater. Sixty-three craters ranging from 2 to 38 km in diameter have been included in the sample. The mean diameter (the average of the north–south, east–west, north-west–south-east and north-east–south-west diameters) the maximum and minimum range of the lobes from the rim of the parent crater, and, where suitable Viking imagery was available, the surface area of the deposit, were measured.

Range of the lobate flows

The mean radial extent of the continuous ejecta from rampart craters, expressed in units of the diameter of the parent crater, has already been described[5]. Prominent lobes were found to extend to three times the range from the rim of the parent crater than the continuous ejecta of mercurian craters, which are considered to be comparable to the martian craters had they too formed on an airless planet[9]. More detailed information pertinent to the mode of formation of the rampart crater lobes can be derived from the distal range of the deposits because this property relates directly to the mobility of the flow at the time of formation.

Figure 1 shows the maximum range of each lobate deposit as a function of the diameter of the parent crater. For primary craters >10 km diameter, an almost linear correlation exists between maximum lobe range and crater diameter, whilst for smaller primaries the maximum lobe range is approximately 15 km from the rim of the parent crater whatever the diameter. Expressing the maximum range of each lobe in units of the primary crater's diameter (Fig. 2) reveals that for craters larger than 10 km diameter, the maximum range of the lobe from the rim crest of the parent crater can be approximated by: $R/D = D/10^{\frac{1}{2}}$ where R is the maximum range of the lobe from the crater rim and D is the diameter of the crater, both in km.

A similar, but numerically different, relationship has also been reported between the volume of material in, and the distance travelled by, terrestrial landslides[10], whilst an in-

Fig. 1 Maximum range of rampart crater lobes as a function of primary crater diameter.

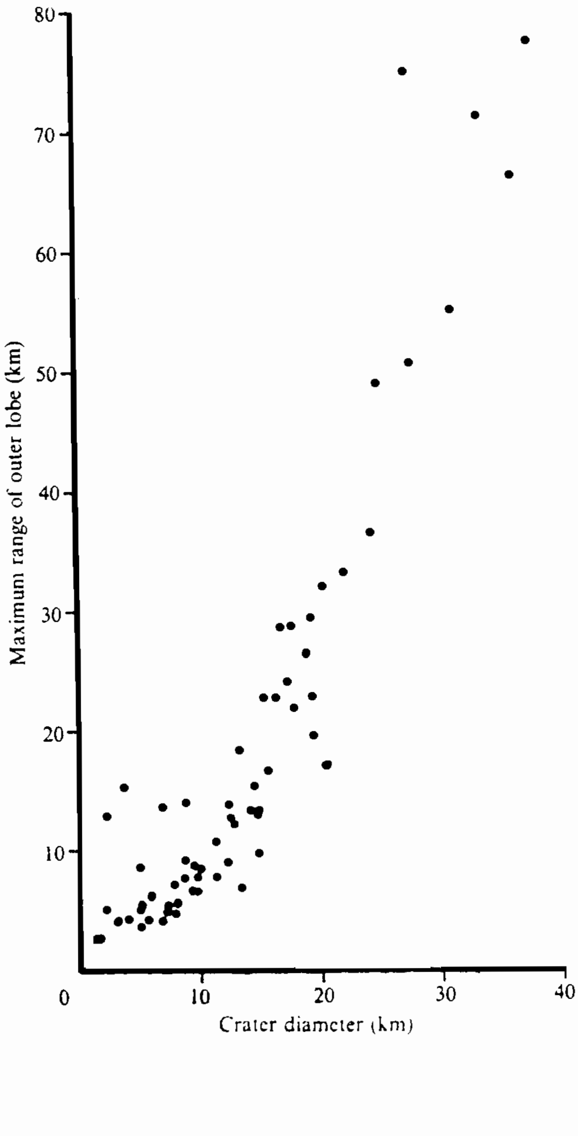

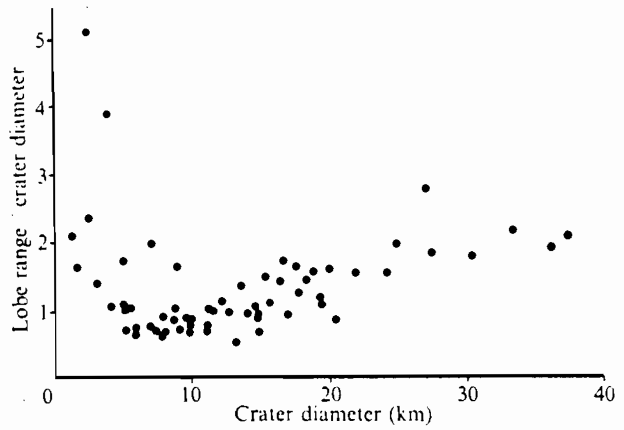

Fig. 2 Maximum range of rampart lobes as a function of primary crater diameter: normalised to the diameter of parent crater. Craters larger than 10 km diameter illustrate a maximum lobe range which approximates to: $L/D = (D/10)^{1/2}$ where L is the lobe range and D the crater diameter.

crease in the mobility of pyroclastic flows may also exist as the volume and 'fall height' of an ignimbrite increases[11]. It seems, therefore, that the increased mobility of the lobes around larger rampart craters is a product of the volume of the material excavated from the crater cavity, rather than being a physical manifestation of a higher flow moisture content.

Craters smaller than 10 km diameter conform to a different relationship: the maximum travel distance of a lobe is limited to no more than 15 km from the rim of the parent crater, but the range is independent of crater diameter. For this size of crater, it is possible that lobe dispersion may be controlled more by the local topography and the structural uplift of the crater rim. Because the lobate flows from these smaller craters are morphologically similar to the flows around large rampart craters, it is believed that they are both part of the same population, although the precise mechanism of lobe formation for small craters is not well understood.

Secondary impact cratering has been suggested as a possible mechanism for the initiation of lobe movement[7]. When large secondary blocks of ejecta impact the surrounding terrain, large quantities of ground moisture may be incorporated in a martian 'muddy base surge' that gains some of its mobility from the moisture-rich tertiary ejecta. It is suggested here and discussed in more detail elsewhere[8], however, that secondary cratering is not the process by which the mobility of the flows is controlled. Stratification within the lobes around many of the larger rampart craters to form two or more near continuous lobes implies more than one period of lobe formation, because the inner lobes appear to over-ride the earlier, more extensive, outer lobes. Size sorting of in-flight ejecta, by atmospheric drag, has been proposed as a possible process by which two or more discrete periods of secondary cratering may occur on Mars[12]. In this model, however, ejecta blocks were considered to travel independently from the point of excavation to the final point of impact, and this bears little relation to the most likely process of ejecta emplacement on Mars because it assumes that the atmosphere is able to move around each block of ejecta. Due to the very high ejecta cloud density/atmospheric density ratio, ejected blocks cannot interact individually with the atmosphere, and little atmospheric deceleration of an ejecta cloud should occur[8], so that the deposition of martian ejecta may be similar to the lunar case[7].

The closest approach to the rim of all the rampart crater lobes (and, where they exist, the inner lobes as well) are shown in Fig. 3 as a function of crater diameter. Also depicted are the distances at which maximum secondary cratering around lunar and mercurian craters is observed[5,9]. It is clear that many of the outer rampart lobes, and all of the inner lobes, originate much closer to the primary crater than the region where maximum secondary cratering occurs. If secondary cratering were the dominant process by which lobes were initiated, the distribution presented in Fig. 3 should not occur until at least 1.4 crater radii from the primary crater because this is the region where the process is predicted to be most influential[5,9]. It is, therefore, unlikely that secondary cratering plays a major part in the process of rampart crater lobe formation.

Surface area of rampart lobes

Photographs of only 14 craters were available for the measurement of the surface area of the rampart lobes. The sample is small because it was considered necessary to have at least 270° azimuthal coverage of the entire ejecta blanket on orthographic, or near vertical, high resolution Viking imagery. Lobe surface area was calculated by tracing the lobe boundary onto a clear acetate overlay and placing this overlay on top of a sheet of graph paper and counting the underlying squares (each of which were of known relative size with respect to the crater being measured). Craters with less than 360° azimuthal coverage were given a scaled lobe surface area. In all cases, only the surface area of the inner lobe (or the single lobe for the smaller craters) was measured, except for two craters where superior photography permitted the outer lobe (Fig. 4*a*) as well as the inner lobe to be included. When the logarithm of the surface area of the lobes is plotted against the logarithm of the crater diameter (Fig. 4) a surprising correlation is revealed. With the exception of the craters *a*, *b* or *c* in Fig. 4, the relationship between the two variables is almost linear: when the crater diameter is plotted as the abscissa the slope of the straight line has a value of 3.06. The exclusion of crater *b* is justifiable because it lies close to the distal end of a large channel system and hence may represent a crater formed in an abnormally moist environment. Crater *c* can also be

Fig. 3 Minimum range of outer (*a*) and inner (*b*) lobes. Also shown are the locations of maximum secondary cratering for the Moon and Mercury[5,9], and the maximum range of the outer lobes given in Fig. 2. It is demonstrated that lobe initiation occurs much closer to the rim crest of the primary crater than the area of maximum secondary cratering, and so lobe formation is unlikely to be dominated by the secondary cratering process.

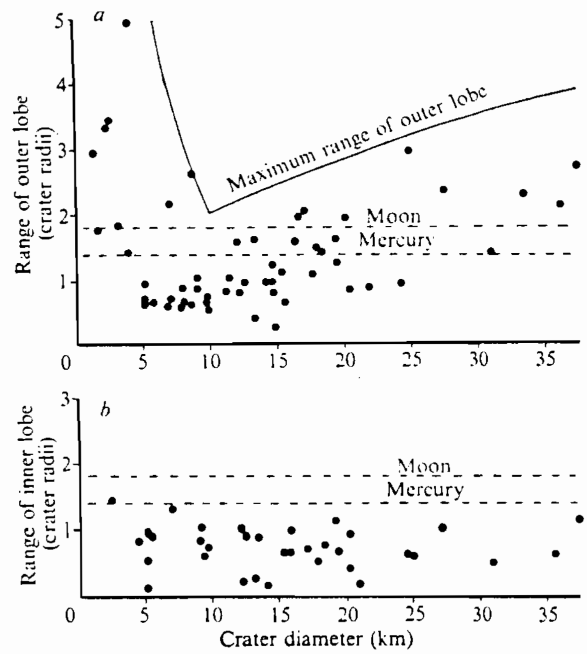

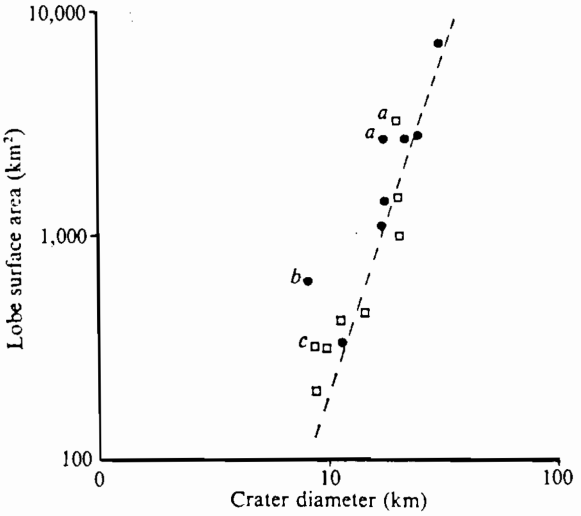

Fig. 4 Rampart lobe surface area as a function of crater diameter. Data derived from two sources: orthographic projections of Viking imagery (●) and near vertical rectilinear prints (□). *a*, Two measurements of the outer lobes of craters, all other values are for the inner lobes of twin-lobed craters and the single lobe for smaller (< 15 km) craters: *b* has an abnormally high (surface area/crater diameter) ratio, due to the proximity of a delta system. *c* is a doublet crater with both craters contributing to the total lobe surface area. Craters *a*, *b* and *c* have been omitted in determining the mean thickness of the lobate deposits. The dashed line corresponds to the function: lobe thickness ∝ crater radius$^{-0.06}$.

excluded because there is a second, smaller primary crater on the lobate deposit of the large primary which has also contributed to the surface area of the entire deposit.

From Fig. 4, we find that the area of the lobe is given by the function $A = 0.152\,D^{3.06}$, where A is the surface area of the lobe in km² and D is the diameter of the crater in km. Because fresh impact craters display a close association between depth and diameter[13,14], it follows that there is some correlation between crater diameter and the volume of the excavated crater cavity (and hence the ejected material). If this volume is given as v, and the crater radius as r, then: $v \propto r^3$. Assuming that the rampart crater lobe forms a layer of mean thickness t and surface area A, it follows that: $A\,t \propto r^3$. From Fig. 4, it is shown that $A \propto r^{3.06}$ and so $t \propto r^{-0.06}$.

It seems, therefore, that the mean thickness of the rampart lobes is nearly independent of crater size, and that some mechanism apart from the cratering event determines the thickness of the lobes. Figure 5 represents the volume of a rampart crater lobe deposit for different estimates of the mean lobe thickness. Also shown are five pairs of data points for five morphologically fresh mercurian craters. The dimensions of these craters were computed by photoclinometric techniques[8] similar to those used by Hapke *et al.*[15] and display similar depth/diameter ratios to those of fresh martian craters[16]. The volume of the excavated crater cavity and the crater rim were calculated for these mercurian craters from the measured profiles using the equations of Pike[17]. It is assumed that mercurian craters are acceptable comparisons with martian craters, because the gravitational fields of the two planets are similar[5,9]. The photoclinometric technique could not be applied to the martian craters due to random photometric variations in the Viking imagery which were induced by the martian atmosphere.

Figure 5 demonstrates that if the 'missing volume' between the volume of the excavated crater cavity and the volume of the crater rim (which represents both the structural uplift and deposited ejecta) is dispersed uniformly around the rampart crater, a mean thickness for the rampart lobes between 30 and 60 m is likely. All five values for the missing volume of the mercurian craters lie within this region. Such a value for the lobe thickness compares favourably with other planetary flow features. The Blackhawk Landslide in Southern California is ~15 m thick[6] and the landslide feature on the rim of the lunar crater Tsiolkovsky is estimated to be ~100 m thick[18].

Conclusions

Rampart craters represent a new category of martian craters. It is assumed here that the main reason for their unusual morphology is the presence of a layer of ground moisture (either a martian aquifer or a layer of permafrost) at the time of crater formation. The increase in the maximum range of the lobes with increasing crater diameter reflects a ground flow process which may have been similar to a mudflow or landslide[10]. The uniformity of the mean lobe thickness for a range of crater diameters precludes a simple ballistic deposition origin for the lobe, and this model is also rejected on the grounds that multiple-lobe initiation is observed to occur very close to the primary crater's rim. Future analysis of rampart craters should re-

Fig. 5 Lobe volume lines (in m for the estimate of the thickness of the lobe) deduced from the relationship shown in Fig. 4. Also shown are the photoclinometrically derived[15] estimates for the crater cavity volume (□) and cavity volume minus rim volume (●) of five morphologically fresh impact craters on Mercury. A mean lobe thickness for all sizes of rampart craters is inferred to be ~30–60 m, as this corresponds to the missing volume of the ejecta from the mercurian craters.

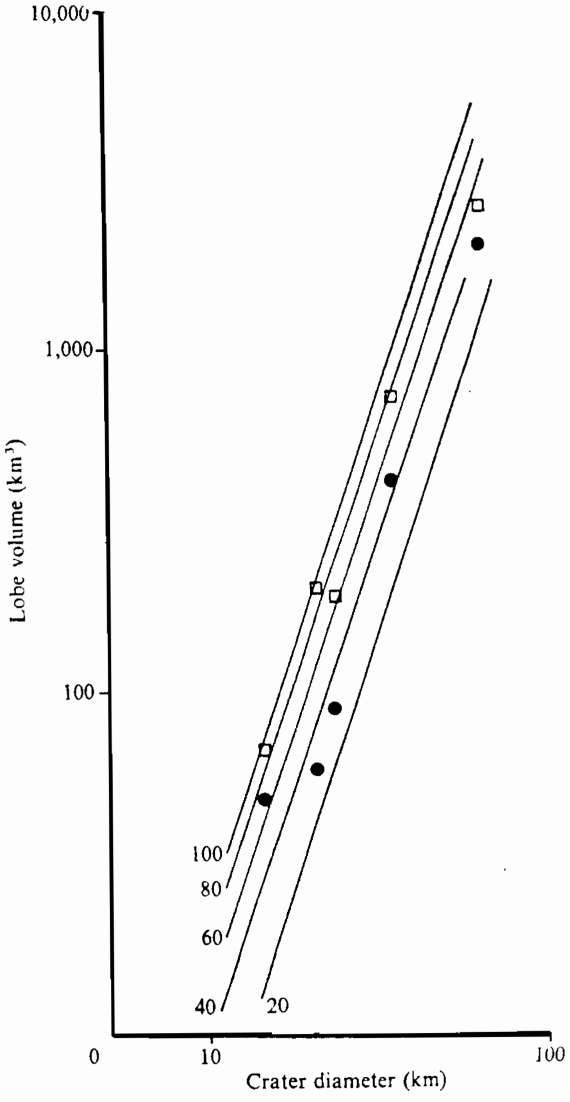

flect the wide variety of possible modes of formation for these features. Results relating to the possibility that these lobes are produced by heating from a hot ejecta blanket emplaced on a layer of permafrost, mass-movement under martian periglacial conditions and the influence of various ground moisture contents on the size of the lobes will be presented in the near future.

This research was carried out during the tenure of a NERC studentship. I thank Drs Wilson and Fielder for their advice and encouragement over the last three years, and the members of the Lunar and Planetary Unit at Lancaster for their helpful suggestions. The work on the Viking data forms part of a joint investigation with the University of London Observatory at Mill Hill.

Received 16 December 1977; accepted 1 February 1978.

1. Carr, M. H. *et al. Science* **193**, 766–776 (1976).
2. McCauley, J. F. *J. geophys. Res.* **78**, 4123–4138 (1973).
3. Arvidson, R. E. *et al. Icarus* **27**, 503–516 (1976).
4. Head, J. W. & Roth, R. in *Symp. planet. Cratering*, Flagstaff Arizona (1976).
5. Carr, M. H. *et al. J. geophys. Res.* **82**, 4055–4065 (1977).
6. Shreve, R. L. *Geol. Soc. Am.* Sp. Pap. No. 108 (1968).
7. Oberbeck, V. R. *Rev. geophys. Space Phys.* **13**, 337–362 (1975).
8. Mouginis-Mark, P. J. thesis, Univ. Lancaster (1977).
9. Gault, D. E., Guest, J. E., Murray, J. B., Dzurisin, D. & Malin, M. L. *J. geophys. Res.* **80**, 2444–2460 (1975).
10. Hsu, K. J. *Geol. Soc. Am. Bull.* **86**, 129–140 (1975).
11. Sparks, R. S. J. *Sedimentology* **23**, 147–188 (1976).
12. Schultz, P. H. & Gault, D. E. *Proc. 8th Lunar Sci. Conf.*, Houston, Texas (1977).
13. Pike, R. J. *The Moon* **15**, 463–477 (1976).
14. Pike, R. J. *Proc. 7th Lunar Sci. Conf. Abstr.* 700–702 (1976).
15. Hapke, B., Danielson, E., Klassen, K. & Wilson, L. *J. geophys. Res.* **80**, 2431–2443 (1975).
16. Burt, J., Veverka, J. & Cook, K. *Icarus* **29**, 83–90 (1976).
17. Pike, R. J. *J. geophys. Res.* **72**, 2099–2105 (1967).
18. Guest, J. E. in *Geology and Physics of the Moon* (ed. Fielder, G.) (Elsevier, Amsterdam, 1971).